Rate Effects Increasing Lateral Capacity of Monopiles

M. M. Wahl & L. Hamre
Det Norske Veritas (DNV), Høvik, Norway

G. R. Eiksund
Norwegian University of Science and Technology (NTNU), Trondheim, Norway

T. I. Tjelta
re:geo (f*ormer Equinor*)*, Stavanger, Norway*

P. Suzuki
Norwegian Geotechnical Institute (NGI), Oslo, Norway

M. Rose
SSE Renewables, Glasgow, Scotland

ABSTRACT: Lateral soil resistance is a key driver for the design of offshore wind monopile foundations but current practice does not explicitly consider the effects of loading rate. This study investigates the effect of loading rate and hence, local strain rate, on clay strength using coupled Eulerian-Lagrangian Finite Element Analyses (FEA). The effect of loading rate on monopile lateral capacity is studied for a representative Ultimate Limit State (ULS) load case at a clay dominated location in the Dogger Bank Offshore Wind Farm. Calibration and validation of the advanced strain softening rate dependent soil model is done by means of laboratory tests and full-scale spudcan penetration tests at different penetration rates. The FEA of the monopile with the rate dependent soil model showed a considerable increase in lateral resistance for the representative ULS load case when compared to a conventional analysis where the rate effect is omitted. This suggests that there may be further room for geometry optimisation if rate effects are accounted for in monopile design.

1 **Introduction**

Monopiles are large diameter piles with relatively small embedment depth to diameter ratio and are the most used foundation type for offshore wind turbines.

The recent Pile–Soil Analysis (PISA) joint industry project investigated the lateral capacity of monopiles to develop design methods suited for monopiles, see e.g. Zdravkovi´c et al. (2020a, b) and Byrne et al. (2020). In the PISA project, lateral load tests were carried out to study monopile capacity under monotonic lateral loading. During one of the tests in clay, the loading rate was unintentionally and dramatically increased which led to a significant increase in resistance. A more controlled second test was conducted to further investigate the observed rate effect. From the two tests it was observed that the pile lateral resistance increased with 33% and 8%, respectively, per $\log_{10}$-cycle increase in loading rate (Byrne et al., 2020). This indicates that monopiles in clay may have significant reserves of strength for high loading rates. These reserves can be utilised in Ultimate Limit State (ULS) design when designing for loads with a short duration, such as wave loads. The authors are not aware of other studies investigating the effect of loading rate on monopile monotonic lateral capacity.

This study is based on full scale spudcan penetration tests at a clay dominated location in the Dogger Bank offshore wind farm area. The main motivation for the tests was to understand the operational strength of clays relative to large foundations such as monopiles. Determining clay strength properties of Dogger Bank clay has proven difficult due to the complicated geological history at the site resulting in complex soil conditions including fissured clay (Yetginer and Tjelta, 2020). The spudcan penetration tests to a depth of 10m-20m below seabed were conducted at different penetration rates, hence the effect of loading rate on penetration resistance can be observed from the measurements. The results from these tests were used to quantify the loading rate effect and to calibrate a strain rate dependent soil model for Finite Element Analyses (FEA). This model was used to study rate effects on the lateral capacity of monopiles, at the example of a clay dominated location at Dogger Bank. This paper is to a large extent based on the master thesis by Wahl (2021).

1.1 *Approach*

The current approach consists of two steps.
Step 1: Large Deformation Finite Element analyses (LD-FEA) were carried out to back-calculate soil strength, strain rate and strain softening properties from the spudcan tests at Dogger Bank. The LD-FEA were conducted using the Coupled Eulerian-Lagrangian (CEL) approach available in Abaqus\Explicit (Abaqus, 2019) with a user defined material model capable of describing strain rate and strain softening effects. To define the soil properties

for the back-calculation, CPT and laboratory data obtained from the Dogger Bank wind project was used.

Step 2: The step 1 material model parameters and analysis methodology were used in monopile pushover analyses. In the analyses, the monopile was pushed over at different rates, enabling the quantification of the rate effect on the global lateral resistance. A typical Dogger Bank monopile was used in these analyses reflecting ULS loading conditions.

2 Strain rate and strain softening effects

The undrained shear strength of clays decreases when subjected to shear strains and remoulding. The ratio of peak or intact and remoulded shear strength typically ranges from 2 to 5 for marine clays (Kvalstad et al., 2001). The decrease of shear strength with increasing shear strain is referred to as strain softening. Accounting for strain softening in FEA is important when modelling large deformations due to the resulting large shear strains, e.g. when modelling spudcan penetration as noted by Hossain and Randolph (2009).

Another property of clays is the rate effect, and it describes how the shear strength of clays are dependent on the rate of applied shear strain. In general, the shear strength increases with increasing shear strain rate and clays typically show an increase in strength of around 5-20 % per $\log_{10}$-cycle increase in loading rate (Casagrande and Wilson, 1951; Dayal and Allen, 1975; Hossain and Randolph, 2009). The effect of strain rate on measured strength in triaxial and DSS tests from several different Norwegian clays is plotted by Lunne and Andersen (2007), and a fitting function to the data has been proposed by Khoa et al. (2019), as shown in Figure 1. The function give $s_u/s_{u,ref}$ as a function of applied strain rate $\dot{\gamma}$ where s_u is the mobilised shear strength and $s_{u,ref}$ is the shear strength measured at the reference strain rate $\dot{\gamma}_{ref}$.

2.1 *Modelling of softening and rate effects*

The used constitutive law is a modified Tresca model which accounts for strain softening and rate effects by modifying the undrained shear strength according to the strain rate and accumulated plastic shear strain with the following expression:

$$s_u = \underbrace{\frac{1}{1+\eta}\left[1+\eta\left(\frac{\max(\dot{\gamma},\dot{\gamma}_{\text{ref}})}{\dot{\gamma}_{\text{ref}}}\right)^{\beta}\right]}_{=f_{\text{rate}}\ \text{(Rate effects)}} \cdot \underbrace{\left[\delta_{\text{rem}}+(1-\delta_{\text{rem}})e^{-3\xi/\xi_{95}}\right]}_{=f_{\text{soft}}\ \text{(Softening effects)}} \cdot s_{u,\text{ref}} \qquad (1)$$

where s_u = undrained shear strength, η = viscous property, β = shear-thinning index, $\dot{\gamma}$ = strain rate, $\dot{\gamma}_{\text{ref}}$ = reference strain rate, δ_{rem} = softening parameter, ξ = cumulative plastic shear strain, ξ_{95} = cumulative plastic shear strain required for 95% remoulding (ductility parameter) and $s_{u,\text{ref}}$ = reference shear strength at the reference shear strain rate before softening.

This material model (Equation 1) is primarily developed at the University of Western Australia (UWA) and is referred to as the UWA-model in this paper. This model or similar models have previously been developed or used by Herschel and Bulkley (1926), Zhou and Randolph (2007), Zhu and Randolph (2011) and Kim et al. (2015).

To model the loading rate in FEA, a normalised velocity v_n is used; using the true velocity directly is too computational expensive:

$$v_n = \frac{v}{L_c \dot{\gamma}_{\text{ref}}} \qquad (2)$$

where v = the true loading rate or velocity and L_c = characteristic length in the physical problem (i.e. spudcan diameter, monopile diameter). v_n is kept constant between the physical problem and the FEA. This approach has previously been used by Hossain and Randolph (2009), Chatterjee et al. (2012) and Khoa et al. (2019) to model rate effects.

3 Back Calculation of Spudcan Penetration

3.1 *Dogger Bank site characterisation*

The Dogger Bank Offshore Wind Farm is located ~130km southwest off the coast of Yorkshire, England. The Dogger Bank area is a topographical high in the middle of the North Sea with complex soil conditions due to a complicated geological history with periods of repeated glaciation. Geological processes like desiccation, ice deformation, erosion and different sedimentation environments have resulted in large soil variability, both laterally and vertically

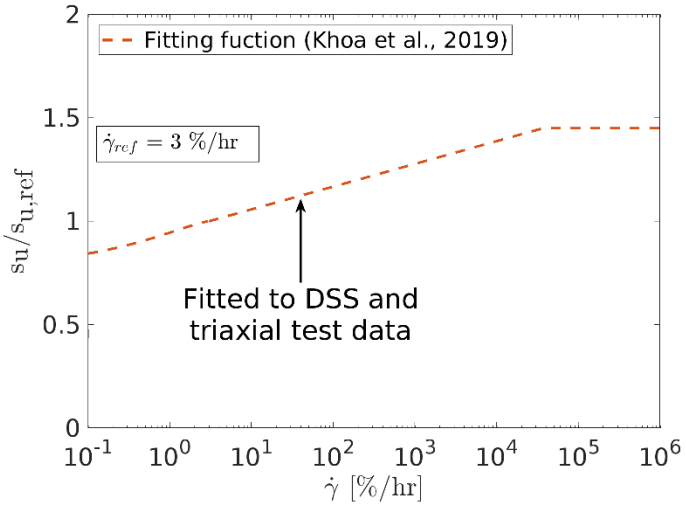

Figure 1: Undrained shear strength as a function of applied strain rate

(Cotterill et al., 2017a, b). In particular, desiccation and freeze-thaw processes have resulted in fissured clay units making it challenging to determine the clay strength due to scale effects.

Marsland (1972) has previously shown that scale effects result in overestimation of strength in the stiff fissured London clay, when determined on small scale samples. Scale effects have also been discussed by Meyerhof (1983) and Lunne et al. (1997). In the Dogger Bank project, it has been observed that small scale laboratory strength determination on the clay units from the site, underestimates the strength for large scale foundations due to relatively small fissure spacing in the clay. Triaxial tests on the clay resulted in N_{kt} in the approximate range 10-50 (Yetginer and Tjelta, 2020).

3.2 *Jacking trials*

The challenge of scale effects motivated the wind farm developer to perform large scale spudcan penetration tests to better understand the operational undrained shear strength of fissured clays relative to large foundations such as monopiles. Jacking trials were performed at Dogger Bank in 2017 and 2020, and succeeded to significantly reduce the N_{kt} range for design. The jacking trial at location DBB-JU1 was considered for back-calculation in this paper. The used four legged jack-up has spudcans with bearing area of 123.5m^2. The maximum achievable pre-load was approximately 123MN. The individual legs are named after their relative position to the jack-up, i.e. SBF, PSF, SBA and PSA (SB = starboard, PS = port side, A = aft, F = front). The spudcan penetration was load controlled and the jack-up rig was capable of continuous penetration, which was utilised to perform tests at high loading rates. At location DBB-JU1, four penetration tests are available, one for each leg. Two of the tests were conducted as regular slow penetration tests, and two tests were conducted with fast penetration rate.

3.3 *Soil conditions at location DBB-JU1*

At the jacking trial location, one cone penetration test (CPT) with pore pressure measurement was carried out at each of the four jack-up legs in addition to one at the centre of the location. The measured corrected cone resistance q_t is shown in Figure 2.

A design q_t profile was established by considering the average resistance from the CPTs and applied in the back-calculation. Using an average profile is justified by the fact that the zone of influence for a CPT is small compared to a spudcan, hence the average profile is believed to be more representative for the spudcan penetration.

The soil conditions consist of a 1m thick surface layer of fine to medium sand overlaying clay with

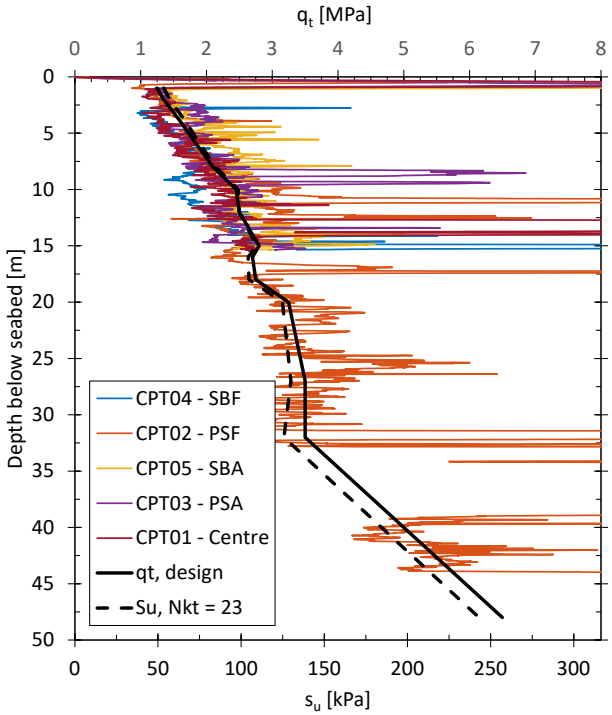

Figure 2: Corrected cone resistance from CPTs at location DBB-JU1 and s_u-profile

frequent sand lenses down to approximately 31m depth. The sand lenses are small compared to the spudcan and it is assumed that the soil will behave as a clay during spudcan penetration. The undrained shear strength of the clay layer is calculated as $(q_t - \sigma_{v0})/N_{kt}$, where σ_{v0} is the overburden stress and N_{kt} is a cone factor. For this study, N_{kt} = 23 has been adopted which is the best estimate based on back-calculations perfomed by the Dogger Bank project. The corresponding s_u-profile is shown in Figure 2.

The softening parameter δ_{rem}, which is describing the post peak strength, was challenging to determine due to the presence of fissures. For this study, δ_{rem} in the range from 0.17 to 1.00 were tested, but δ_{rem} = 0.25 was selected for back-calculation.

The initial stresses of the soil have little influence on the spudcan penetration resistance because the resistance is mostly governed by plastic deformation. The selected soil parameters for the back calculation are summarised in Table 1.

3.4 *LD-FE model for spudcan penetration*

The CEL approach is used to model the large deformations during spudcan penetration. CEL combines the advantages of Lagrangian meshes, typically used in geotechnical and structural engineering, and Eulerian meshes.

With an Eulerian mesh, the nodes of an element are stationary in space, whereas the material points move in space through the mesh. Hence, the mesh will not be distorted if the material deforms severely and solution accuracy is maintained, as opposed to a Lagrangian mesh (Belytschko et al., 2014). The CEL

Table 1: Adopted soil properties for location DBB-JU1. z_{top} and z_{bot} refer to depth to the top and bottom of the layers below the seabed.

z_{top} [m]	z_{bot} [m]	Soil type [-]	γ' [kN/m^3]	E	ν^* [-]	δ_{rem} [-]	ξ_{95} [-]	K_0 [-]	φ^{**} [deg]	N_{kt} [-]
0	1	Sand	9	35MPa	0.3	-	-	1	33	-
1	30	Clay	9	200s_u	0.5	0.25	1	1	-	23

$^*\nu$ = Poisson's ratio. $^{**}\varphi$ = constant volume fiction angle.

approach has been used and validated for geotechnical problems in several publications (Qiu et al., 2011; Tho et al., 2012; Dutta et al., 2015; Kim et al., 2015)

To account for softening and rate effects, the UWA-soil model (Equation 1) is used to model the clay constitutive behaviour and implemented in Abaqus\Explicit. ξ is calculated as $\xi = \sum_t(\Delta\varepsilon_{eq})$ were $\Delta\varepsilon_{eq}$ is the incremental equivalent plastic strain in the von Mises yield criterion and t is time. The strain rate is calculated as $\dot{\gamma} = \Delta\varepsilon_{eq}/\Delta t$. In addition, a cap $f_{\text{rate}}^{\max}$ for the rate effect, f_{rate}, is implemented such that $f_{\text{rate}} \leq f_{\text{rate}}^{\max}$. The sand is modelled with the Mohr-Coulomb material model available in Abaqus (2019).

The spudcan FEA in Abaqus\explicit was modelled in 3D, where the Eulerian soil is modelled as a quarter cylinder with radius of 30m. The vertical boundaries are laterally fixed normal to the boundaries and the bottom boundary is fixed in the vertical direction.

The spudcan is modelled as a solid weightless rigid body. The soil-structure interface strength is set equal to the average remoulded strength over the depth interval 0-15m (15m being the maximum penetration depth), as modelling a varying interface strength is not currently possible when using Abaqus CEL. The FE model is shown in Figure 3.

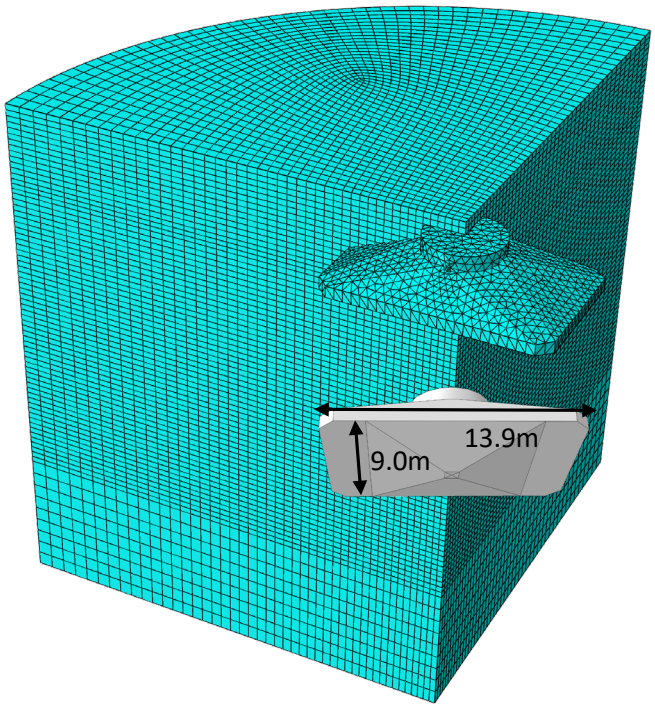

Figure 3: FE-model with mesh discretisation and spudcan bottom view. Note that the full spudcan model is shown for illustration.

In the FEAs, the spudcan is prescribed a constant penetration velocity and the required reaction force is recorded to obtain the load penetration response. A Butterworth filter (Tseng and Lee, 2017) is applied in the post processing to remove numerical oscillations from the resistance curve.

The FE-model was verified in a comprehensive convergence study where the effect of the following model properties on the solution accuracy was checked; soil domain size, mesh density, analysis penetration velocity (dynamic effects), soil-spudcan contact formulation (interface strength) and clay rigidity index (E/s_u). A sufficiently converging solution was obtained with the selected model properties, as described above, except for the adopted mesh density and analysis penetration velocity. The adopted mesh density and velocity gave an overestimation in penetration resistance in the order of 6%, but with an acceptable computational time. The convergence study is further described in Wahl (2021).

3.5 *Calibration of rate and softening parameters from spudcan penetration tests*

To obtain a reference shear strength profile, the best estimate N_{kt} equal to 23 from the spudcan back-calculations by NGI was used. Next, different values of δ_{rem} were tested to obtain a good match with the slow spudcan penetration tests. Thereafter, different values for the rate effect parameters, i.e. η, β and $f_{\text{rate}}^{\max}$, were tested to obtain a good match with the fast penetration tests. Accounting for strain softening in the spudcan back-calculation on Dogger Bank clay is challenging since the strength and softening properties of the clay are uncertain and changing N_{kt}, δ_{rem} and ξ_{95} have a similar effect on the penetration resistance. Hence, the same response can be obtained for different combinations of the three parameters. Soil parameters as presented in Table 1 are adopted in the FEA and the reference shear strain rate is taken as $\dot{\gamma}_{ref}$ = 3%/hr as typically used in triaxial testing.

Figure 4 is showing measured spudcan load-penetration response (slow and fast tests) from DBB-JU1 together with the results from FE-analyses. The plotted penetration depth D is referring to the depth of maximum spudcan bearing area. The penetration rates from the spudcan tests are shown in Figure 5. Since it is not possible to model a

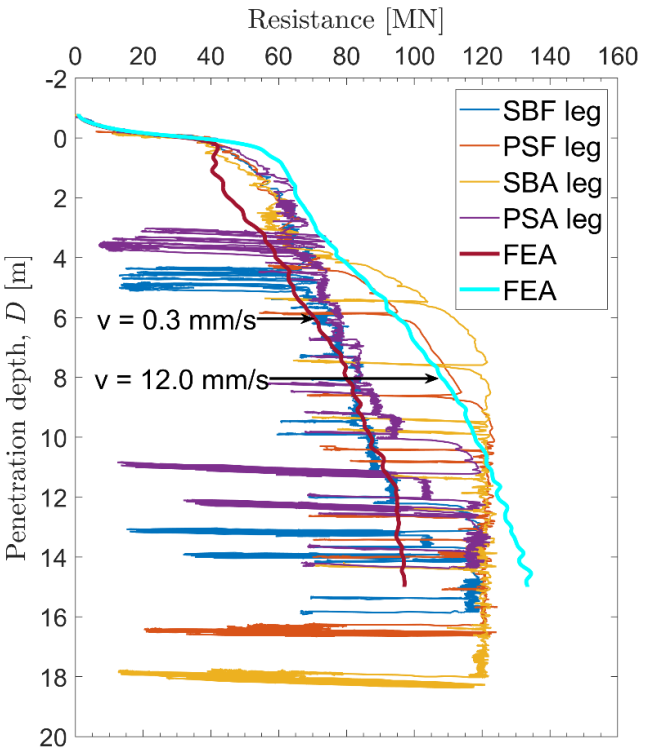

Figure 4: Measured and calculated spudcan load-penetration response

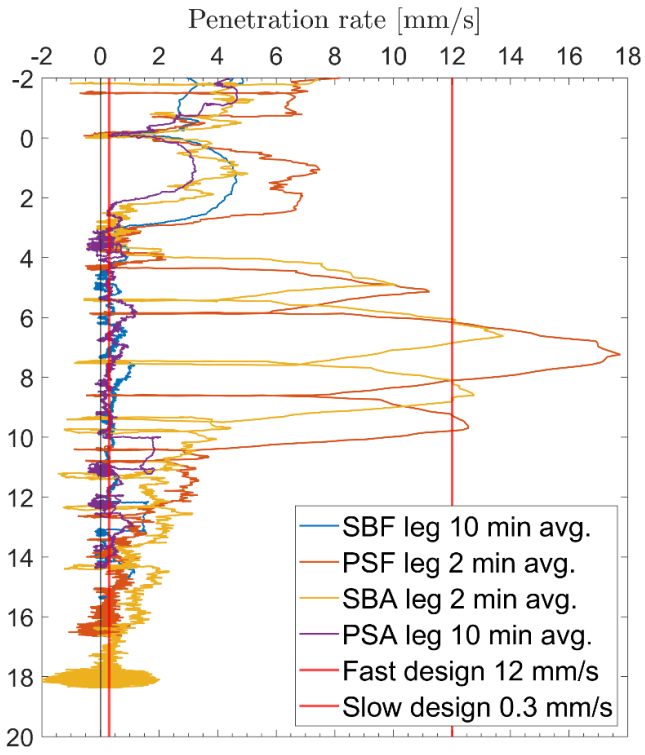

Figure 5: Measured penetration rate during the spudcan tests

changing penetration rate in the adopted FEA approach, 0.3mm/s and 12mm/s were selected for analysis.

A clear rate effect is observed with an increase in resistance in the order of 30-40% from the slow to the fast penetration test, which corresponds to approximately 22% increase per log-cycle increase of loading rate. This is close to the expected range for clays based on small scale laboratory testing.

Strain softening and rate parameters were selected by trial and error guided by available data. The final adopted parameters are $\delta_{rem} = 0.25$, $\xi_{95} = 1$, $\eta = 0.5$, $\beta = 0.4$ and $f_{rate}^{max} = 6$. With these parameters, the FEA gave reasonably good agreement with the measurements when considering the variability in recorded resistance, soil properties and penetration rate. A sensitivity study, where the different parameters of the soil model were varied, has been conducted and documented in Wahl (2021).

To validate the back-calculated rate effect parameters, they were tested in an FE-model of a standard undrained triaxial compression test on a 54mm clay specimen. The soil specimen was modelled in Abaqus\Explicit with approximately 66 000 Eulerian elements and the UWA soil-model. Documentation and verification of the triaxial FE-model can be found in Wahl (2021). The triaxial model simulated strain rates of 3%/hr and 3600%/hr. The resulting global rate effect from the two tests is shown in Figure 6 together with the rate effect fitting function, which is based on laboratory triaxial tests. Good agreement between the FE results and lab-based curve is observed. It should be stressed that the rate effect parameters that are used in the FE-triaxial test are solely back-calculated from the spudcan penetration tests, and the FE triaxial verification was done after the back calculation. Hence, the good agreement is not due to unintended bias. This is a strong indication that the parameters give a rate effect which is realistic. Based on the above validation it is concluded that the obtained rate effect parameters are suited for studying rate effects on monopile lateral capacity.

4 Rate Effects on Monopile Lateral Capacity

4.1 *Problem formulation*

To investigate how strain or loading rate effects affect the lateral capacity of wind turbine supporting monopiles, FE analyses of a laterally loaded monopile in clay with varying loading rates are performed. The main objective of the FEA is to investigate the effect of loading rate for a realistic Dogger Bank Ultimate Limit State (ULS) design case. In the considered design case, the monopile is pushed to failure by a single wave mobilising the ULS resistance of the soil. In this case, the pile velocities are large, leading to large strain rates in the soil with accompanying strain rate effects. The embedment depth to pile diameter L/D_p-ratio is taken as 3.5 with D_p = 8.6 m. The force resultant of the wave load is applied 55m above the seabed and the wave period T is 12s.

The CEL approach and the UWA model is used in the monopile pushover analyses as the rate effect parameters was calibrated with the same approach.

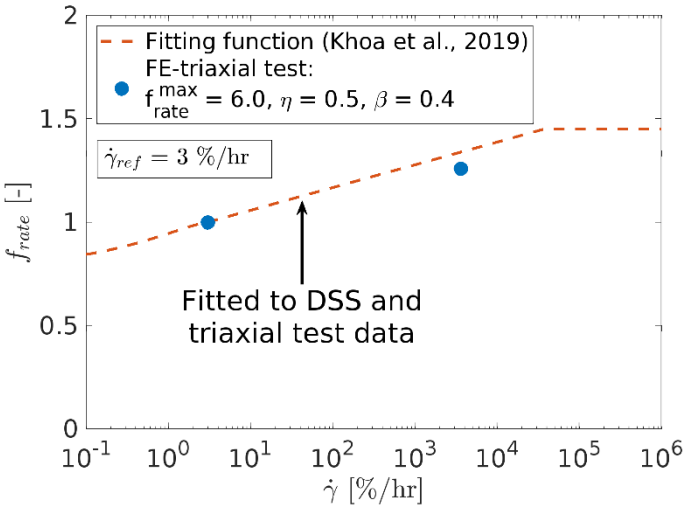

Figure 6: Comparison of strain rate effects measured in real and in FE-simulations of a triaxial compression tests

The Dogger Bank project has previously concluded that strength properties back-calculated from spudcan tests are applicable to laterally loaded monopiles (Yetginer and Tjelta, 2020).

4.2 *Adopted soil parameters*

The modelled soil consists of a uniform clay layer with increasing shear strength with depth, similar to the profile at test location DBB-JU1, previously described in Table 1. The adopted s_u-profile is shown in Figure 2. The sand layer from 0-1m depth is replaced by a homogeneous clay layer with the same properties as the clay at 1m depth.

The adopted elastic stiffness of $200s_u$ is low, therefore, the initial lateral response of the monopile, in the elastic domain, may be too soft, but the ultimate resistance should not be affected. Furthermore, the modelled rate effect is a function of the plastic strain rate, hence, the calculated rate effects is not affected by the low stiffness. For the strain rate and softening effects, parameters determined from the spudcan back-calculation are used, i.e. δ_{rem} = 0.25, ξ_{95} = 1, η = 0.5, β = 0.4 and f_{rate}^{max} = 6.

4.3 *FE-model for monopile push-over analyses*

The FE-model consists of a cylindrical Eulerian soil domain with an embedded monopile, modelled with Lagrangian elements. The radius of the soil domain is set equal to $4D_p$ which is verified to be sufficiently large to avoid boundary effects on the lateral capacity (Wahl, 2021). The embedment depth of the monopile is set to $3.5D_p$, and the soil continuum extends $2D_p$ below the pile tip. To allow for free soil heave during the analysis, a 2m thick layer of void elements is added on top of the soil. The monopile extends 55m above the seabed where the lateral displacement or velocity is applied, and the corresponding reaction force is measured. The monopile is modelled as a rigid body, which is considered a reasonable simplification given that the purpose was to study the relative effect of loading rates. The monopile is assumed weightless in the soil. The soil-structure interface strength is set equal to the average remoulded strength over the monopile embedment depth. The model is shown in Figure 7. It is worth noting that the used contact formulation is not able to transfer tensile stresses between the soil and the pile wall. A gap up to ~20m deep will form behind the pile when it is displaced laterally. Additional capacity from the active wedge is not included.

In the FEA the monopile top is prescribed a constant lateral velocity and the required reaction force is recorded. The reference shear strain rate $\dot{\gamma}_{ref}$ = 3%/hr as previously used.

4.4 *Monopile push-over FE-analyses*

To model the considered design case where an extreme wave pushes the monopile to the ultimate capacity, an equivalent pile top velocity v needs to be established. It is assumed that the wave load is varying as a harmonic function, hence the maximum load will be reached after t = T/4 or 3s. It is further assumed that the maximum load is reached after the monopile has rotated 5°, which is based on preliminary analyses without strain softening and rate effects. This results in an equivalent pile top velocity of 2.2m/s for ULS. The PISA load tests had a lateral ground velocity of D_p/300/min for most loading steps, equivalent to a pile top velocity of 0.0017m/s in this case. This loading rate was intended to be sufficiently slow to avoid any rate effects (Byrne et al., 2020), and this loading rate will also be considered in the FEA. Additionally, pile top velocities of 0 (no rate effect), 0.1m/s and 1.0 m/s were analysed.

Rotation versus mobilised moment resistance at seabed from the monopile pushover analyses are shown in Figure 8. The ultimate capacity is reached at around 5-6° pile rotation or around 2m displacement at seabed for the three largest loading rates. For the two lowest loading rates, the peak resistance is reached after approximately 2° rotation or 1.0 m of ground displacement and after this, the resistance slightly decreases due to softening.

When increasing the pile top velocity, v, from 0.0017m/s to 2.2 m/s, i.e. from almost static to the ULS design case loading rate, the resistance is increased by 35% at 3° rotation. This corresponds to 11% increase in resistance per $\log_{10}$-cycle increase in loading rate. For loading rates of 0.1 and 2.2m/s at 3° rotation, an increase of 16% per log-cycle is found. Thus, the increase in resistance it not directly proportional to the logarithm of loading rate increase for this model. The observed rate effect is within the range of measured rate effects in the PISA tests which were 8% to 33% increase in resistance per log-cycle. Moreover, it is within the typical range for clay, i.e. from 5-20%. Hence, it is seen that rate

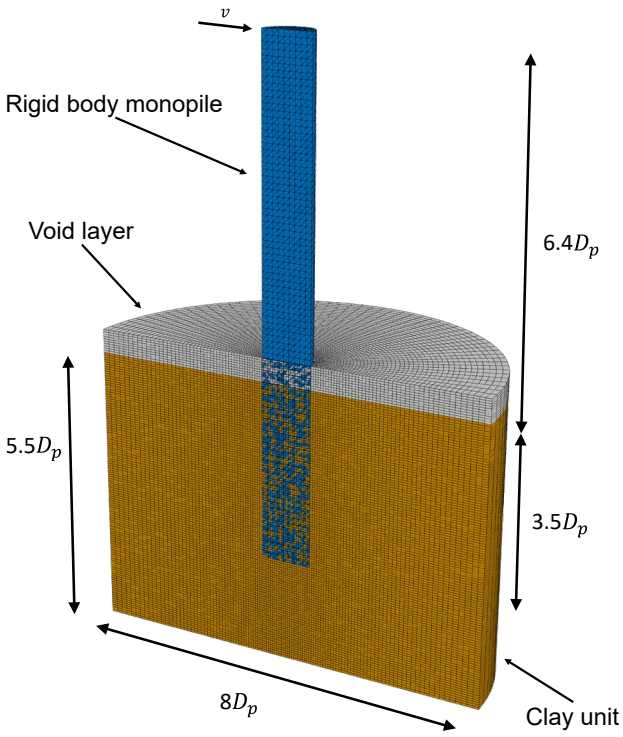

Figure 7: FE-model used for monopile pushover analyses

effects can give a substantial increase in lateral resistance for high loading rates. The considered ULS loading rate may reduce for stiffer soils. However, significant rate effects (approximately an increase of 26%) are also seen for a loading velocity of 1.0 m/s which is approximately half of the ULS loading rate.

In the FEAs, rate effect parameters for the UWA-model, calibrated against spudcan penetration tests, were used. These rate effect parameters, when applied in an FE-model of a triaxial test, gave similar rate effects as observed in physical small scale triaxial tests, see Figure 6. The fact that these parameters can predict rate effects for both large- and small-scale testing, when applied in the current modelling approach, strengthen their validity and supports the rate effect found in the monopile FEA. It is also intriguing to observe that, in general, the magnitude of the rate effect measured in small scale laboratory tests is similar to the magnitude measured in the PISA pile test and large scale spudcan tests. This implies that rate effects measured in the laboratory can be trusted to also apply to large scale foundation design. Rate effects are partially included by the industry when cyclic element tests are used as basis for the design, However, the specific effect of strain rate is not the focus of the cyclic degradation approach and further research may be needed to verify strain rate effects for design.

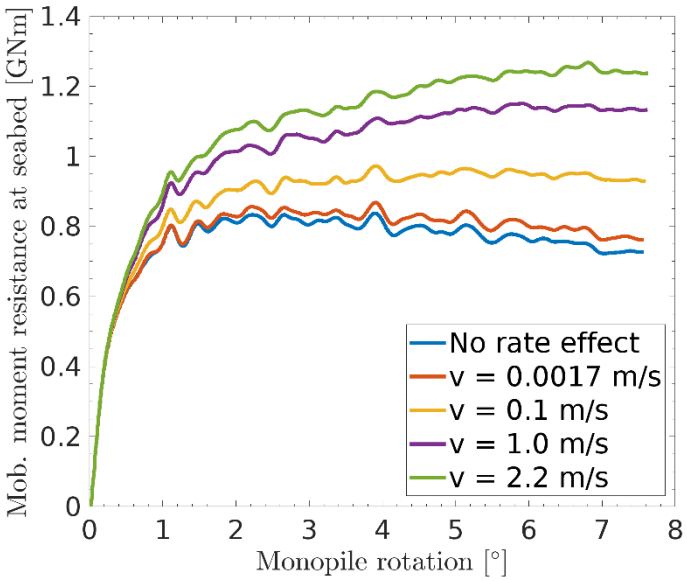

Figure 8: Mobilised moment resistance at seabed versus rotation for different pile top lateral velocities. 1° rotation corresponds to approximately 0.36m lateral displacement at seabed.

5 Concluding remarks

The inclusion of strain rate effects commensurate with a design wave load will increase the lateral capacity of offshore wind turbine monopiles. This determination has been made by performing finite element analyses with a strain softening rate dependent soil model, and model calibration provided by back-calculating rate effect parameters from spudcan penetration tests. The parameters were in turn validated through simulating a triaxial compression test using FEA and comparing to published laboratory data.

It was observed that the penetration resistance in the spudcan tests increased with 30-40% for high loading rates equivalent to approximately 22% increase in resistance per log-cycle increase in loading rate. This is close to expected values for clay.

When using the back-calculated rate effect parameters in finite elements push-over analyses of a monopile with different loading rates, this resulted in a significant increase in lateral resistance due to rate effects. For the loading rate corresponding to a realistic ULS design case, the increase in lateral resistance was 35%. The obtained rate effect was between 11 and 16% increase in resistance per $\log_{10}$-cycle increase in loading rate. The observed rate effect in the spudcan field tests and the calculated rate effect for the monopile is within the range found in the PISA tests, hence confirming the PISA results.

It is seen that calibrating a soil model against full-scale spudcan tests gives soil model parameters that can reasonably well predict rate effects observed in small scale triaxial tests. This implies that rate effects determined in the laboratory can be used for large scale foundation design. In addition, it is well known that in cyclic element tests, carried out at 10s

per cycle, the strength at N = 1 cycle is higher than for a monotonic test on the same material.

Based on the above, it can be concluded that a rate effect of 10% strength increase per $\log_{10}$-cycle or more can be relied upon in large foundation design for a variety of clay types, also for the complex Dogger Bank clay. If rate effects can be adopted in monopile design, this can lead to shorter monopiles.

Further studies are needed to verify the current strain rate effects for industry use. It should also be investigated if rate effects impact the soil stiffness which is an important parameter for monopile design. More full scale or prototype field tests like in PISA would provide valuable information.

6 Acknowledgement

The authors would like to thank Equinor and SSE Renewables for providing jacking trail and soil data from the Dogger Bank project. The authors also gratefully acknowledge the valuable assistance with FE-modelling provided by Miguel Costas and Huynh D.V. Khoa.

7 References

Abaqus (2019). Abaqus version R2019x User'sManuals. Dassault Systèmes.

Belytschko, T., W. K. Liu, B. Moran, and K. I. Elkhodary (2014). Nonlinear Finite Elements for Continua and Structures, 2nd Edition. USA, Beaverton: John Wiley & Sons, Ltd. ISBN: 978-1- 118-63270-3.

Byrne, B. W., R. A. McAdam, H. J. Burd, W. J. A. P. Beuckelaers, K. G. Gavin, G. T. Houlsby, et al. (2020). Monotonic laterally loaded pile testing in a stiff glacial clay till at Cowden. Géotechnique, 70(11), 970–985.

Casagrande, A. and S. D. Wilson (1951). Effect of Rate of Loading on the Strength of Clays and Shales at Constant Water Content. Géotechnique, 2(3), 251–263.

Chatterjee, S., M. Randolph, and D. White (2012). The effects of penetration rate and strain softening on the vertical penetration resistance of seabed pipelines. Géotechnique, 62(7), 573–582.

Cotterill, C., E. Phillips, L. James, C.-F. Forsberg, and T. I. Tjelta (2017a). How understanding past landscapes might inform present-day site investigations: a case study from Dogger Bank, southern central North Sea. Near Surface Geophysics, 15(4), 403–414.

Cotterill, C. J., E. Phillips, L. James, C. F. Forsberg, T. I. Tjelta, G. Carter, et al. (2017b). The evolution of the Dogger Bank, North Sea: A complex history of terrestrial, glacial and marine environmental change. Quaternary Science Reviews, 171, 136–153.

Dayal, U. and J. H. Allen (1975). The Effect of Penetration Rate on the Strength of Remolded Clay and Sand Samples. Canadian Geotechnical Journal, 12(3), 336–348.

Dutta, S., B. Hawlader, and R. Phillips (2015). Finite element modeling of partially embedded pipelines in clay seabed using Coupled Eulerian–Lagrangian method. Canadian Geotechnical Journal, 52(1), 58–72.

Herschel, W. and R. Bulkley (1926). Measurement of consistency as applied to rubber-benzene solutions. Am. Soc. Test Proc. Vol. 26. 2, 621–633.

Hossain, M. S. and M. F. Randolph (2009). Effect of Strain Rate and Strain Softening on the Penetration Resistance of Spudcan Foundations on Clay. International Journal of Geomechanics, 9(3), 122–132.

Khoa, H. D. V., H. P. Jostad, and H. K. Engin (2019). Improvement of NT-bar Evaluation in Clays Using Large Deformation FE Method. Proceedings of the 1st Vietnam-Symposiumon Advances in Offshore Engineering. Springer Singapore, 137–143.

Kim, Y., M. Hossain, D. Wang, and M. Randolph (2015). Numerical investigation of dynamic installation of torpedo anchors in clay. Ocean Engineering, 108, 820–832.

Kvalstad, T., F. Nadim, and C. Arbitz (2001). Deepwater Geohazards: Geotechnical Concerns and Solutions. Houston: Proc., Offshore Technology Conf.

Lunne, T. and K. Andersen (2007). Soft Clay Shear Strength Parameters For Deepwater Geotechnical Design. Proc., 6th Int. Offshore Site Investigation and Geotechnics Conf.: Confronting New Challenges and Sharing Knowledge, 151–176.

Lunne, T., P. Robertson, and J. Powell (1997). Cone penetration testing in geotechnical practice. London: Blackie. Chap. 5.4.2, p. 66. ISBN: 0751403938.

Marsland, A. (1972). Clays subjected to in situ plate tests. Ground Engineering, 5(6), 24–31.

Meyerhof, G. G. (1983). Scale Effects of Ultimate Pile Capacity. Journal of Geotechnical Engineering, 109(6), 797–806.

Qiu, G., S. Henke, and J. Grabe (2011). Application of a Coupled Eulerian–Lagrangian approach on geomechanical problems involving large deformations. Computers andGeotechnics, 38(1), 30–39.

Tho, K. K., C. F. Leung, Y. K. Chow, and S. Swaddiwudhipong (2012). Eulerian Finite-Element Technique for Analysis of Jack-Up Spudcan Penetration. International Journal of Geomechanics, 12(1), 64–73.

Tseng, C.-C. and S.-L. Lee (2017). Closed-form designs of digital fractional order Butterworth filters using discrete transforms. Signal Processing, 137, 80–97.

Wahl, M. M. (2021). Rate Effects Increasing Lateral Capacity of Monopiles. Based on Spudcan Penetration Tests. Master's thesis. The Norwegian University of Science and Technology.

Yetginer, G., T. I. Tjelta (2020). Bridging knowledge between old and new energy projects. 4th International Symposium on Frontiers in Offshore Geotechnics (postponed), 84-119.

Zdravkovi´c, L., R. J. Jardine, D. M. G. Taborda, D. Abadias, H. J. Burd, B. W. Byrne, et al. (2020a). Ground characterisation for PISA pile testing and analysis. Géotechnique, 70(11), 945–960.

Zdravkovi´c, L., D. M. G. Taborda, D. M. Potts, D. Abadias, H. J. Burd, B. W. Byrne, et al. (2020b). Finite-element modelling of laterally loaded piles in a stiff glacial clay till at Cowden. Géotechnique, 70(11), 999–1013.

Zhou, H. and M. F. Randolph (2007). Computational Techniques and Shear Band Development for Cylindrical and Spherical Penetrometers in Strain-Softening Clay. International Journal of Geomechanics, 7(4), 287–295.

Zhu, H. and M. F. Randolph (2011). Numerical analysis of a cylindermoving through rate-dependent undrained soil. Ocean Engineering, 38(7), 943–953